Inorg. Chem. **2002**, *41*, 3353–3358

Synthesis, Crystal Structure, and Photoelectric Properties of $Re(CO)_3ClL$ (L = 2-(1-Ethylbenzimidazol-2-yl)pyridine)

Kezhi Wang,*,† Ling Huang,‡ Lihua Gao,§ Linpei Jin,† and Chunhui Huang*,‡

Department of Chemistry, Beijing Normal University, Beijing 100875, P.R. China, State Key Laboratory of Rare Earth Materials Chemistry and Applications and the University of Hong Kong Joint Laboratory on Rare Earth Materials and Bioinorganic Chemistry, Peking University, Beijing 100871, P.R. China, and College of Chemistry and Environmental Engineering, Beijing Technology and Business University, Beijing 100037, P.R. China

Received July 10, 2001

A novel Re(I) complex, $Re(CO)_3ClL$ (L = 2-(1-ethylbenzimidazol-2-yl)pyridine), has been synthesized and structurally characterized by single-crystal X-ray diffraction analysis. Crystal data for $C_{17}H_{13}ClN_3O_3Re$: space group, orthorhombic, *Pbca*; $a = 12.713(6)$ Å; $b = 15.103(7)$ Å; $c = 18.253(8)$ Å; $Z = 8$. Stable vacuum vapor deposition of the Re complex has been verified by UV–vis and infrared spectroscopy. A two-layer electroluminescent device with configuration of ITO/TPD/$Re(CO)_3ClL$/$Mg_{0.9}Ag_{0.1}$/Ag has been fabricated, which gave a turn-on voltage of as low as 3 V and a maximum luminance of 113 cd/m^2 at a bias voltage of 10.5 V, and confirmed that the Re complex can function as a bright orange-red emitter and an electron transport material in an electroluminescent device.

Introduction

Luminescent Ru(II) and Re(I) metal complexes have attracted considerable attention due to their intriguing photophysical, photochemical, and excited state redox properties, and potential applications in photonic and photoelectronic devices.[1,2] Recently there has been growing interest in electroluminescent (EL) devices with luminescent metal complexes as emitting layers since the first report on an organic EL device based on tris(8-hydroxyquinolinato)-aluminum (AlQ).[3] The luminescent metal complexes were usually introduced into EL devices as light-emitting layers by means of spin-coating, vacuum-depositon, Langmuir−Blodgett (LB), and self-assembling techniques. For obvious reasons, vacuum vapor deposition is the most appealing technique for making practical devices. Although many families of luminescent metal complexes have been reported for electroluminescent devices, e.g., Eu(III),[4] Tb(III),[5] Zn(II),[6] Ru(II),[7] Pt(II),[8] Rh,[9] and Re(I) complexes,[10] novel and vacuum volatile complexes are relatively scarce. Here we report a novel Re(I) complex capable of being vacuum-deposited as the emitting layer of an electrolumnescent device. The optical and X-ray crystal structure characterization and the electroluminescent properties of the Re(I) complex are reported.

Experimental Section

Materials. $Re(CO)_5Cl$ (98%+) was used as purchased from Aldrich Chemical Co. 2-(1-Ethylbenzimidazol-2-yl)pyridine (L) was

* To whom correspondence should be addressed. E-mail: kzwang@bnu.edu.cn (K.W.). Fax: 86-10-62200567.

† Beijing Normal University.

‡ Peking University.

§ Beijing Technology and Business University.

(1) Balzani, V.; Scandola, F. *Supramolecular Photochemistry*; Ellis Horwood: Chichester, 1991.

(2) (a) Yam, V. W.-W.; Wang, K. Z.; Wang, C. R.; Yang, Y.; Cheung, K. K. *Organometallics* **1998**, *17*, 2440. (b) Yam, V. W.-W.; Lau, V. V.-Y.; Wang, K. Z.; Cheung, K. K.; Huang, C. H. *J. Mater. Chem.* **1998**, *8*, 89.

(3) Tang, C. W.; VanSlyke, S. A. *Appl. Phys. Lett.* **1987**, *51*, 913.

(4) (a) Kido, J.; Hayase, H.; Hongawa, K.; Nagai, K.; Okuyama, K. *Appl. Phys. Lett.* **1994**, 65, 2124. (b) Huang, L.; Wang, K. Z.; Huang, C. H.; Li, F. Y.; Huang, Y. Y. *J. Mater. Chem.* **2001**, *11*, 790. (c) Gao, X. C.; Cao, H.; Huang, C. H.; Umitani, S.; Chen, G. Q.; Jiang, P. *Synth. Met.* **1999**, *19*, 127. (d) Yu, G.; Liu, Y. Q.; Wu, X.; Zhou, D. B.; Li, H. Y.; Jin, L. P.; Wang, M. Z. *Chem. Mater.* **2000**, *12*, 2537. (e) Hu, W. P.; Matsumura, M.; Wang, M. Z.; Jin, L. P. *Appl. Phys. Lett.* **2000**, *77*, 4271.

(5) Gao, X. C.; Cao, H.; Huang, C. H.; Li, B. G. *Appl. Phys. Lett.* **1998**, *72*, 2217.

(6) Thomson, D. L.; Papadimitrakopoulos, F. *Polym. Prepr.* **1997**, *38*, 398.

(7) (a) Lee, J.-K.; Yoo, D.; Rubner, M. F. *Chem. Mater.* **1997**, *9*, 1710. (b) Gao, F. G.; Bard, A. J. *J. Am. Chem. Soc.* **2000**, *122*, 7426.

(8) Baldo, M. A.; O'Brien, D. F.; You, Y.; Shoustikov, A.; Sibley, S.; Thompson, M. E.; Forrest, S. R. *Nature* **1998**, *395*, 151.

(9) (a) Baldo, M. A.; Lamansky, S.; Burrows, P. E.; Thompson, M. E.; Forrest, S. R. *Appl. Phys. Lett.* **1999**, *75*, 4. (b) Tstsui, T.; Yang, M.-J.; Yahiro, M.; Nakamura, K.; Watanabe, T. *Jpn. J. Appl. Phys.* **1999**, *38*, L1502.

(10) (a) Li, Y.; Liu, Y.; Guo, J.; Wu, F.; Tian, W.; Li, B.; Wang, Y. *Synth. Met.* **2001**, *118*, 175. (b) Gong, X.; Ng, P. K.; Chan, W. K. *Adv. Mater.* **1998**, *10*, 1337. (c) Li, Y.; Wang, Y.; Zhang, Y.; Wu, Y.; Shen, J. *Synth. Met.* **1999**, *99*, 257.

10.1021/ic0107330 CCC: $22.00
Published on Web 05/22/2002

synthesized according to a modified method we published before.[4b] Indium−tin−oxide (ITO) (150-nm thickness, sheet resistance of 15 Ω/cm^2) coated glass plates supplied by China Southern Glass Holding Co., Ltd., were cleaned immediately before use.[4b]

Synthesis of Re(CO)$_3$ClL (L = 2-(1-Ethylbenzimidazol-2-yl)-pyridine). L (76 mg, 0.34 mmol) and Re(CO)$_5$Cl (120 mg, 0.33 mmol) were refluxed in 15 mL of benzene for 6 h. After cooling to room temperature, the solvent was removed in a water bath under reduced pressure. The resulting yellow solid was twice recrystallized from a dichloromethane−hexane solution. Yield: 141 mg (81%). Anal. Calcd for $C_{17}H_{13}ClN_3O_3Re$: C, 38.60; H, 2.48; N, 7.94. Found: C, 38.63; H, 2.58; N, 7.83. ^{1}H NMR (CDCl$_3$, 400 Mz): δ 1.71 (t, 3H, −CH$_3$), 4.71 (q, 2H, −CH$_2$−), 7.56 (m, 4H, aromatic), 8.14 (m, 3H, aromatic), 9.24 (m, 1H, aromatic). Mp >280 °C.

Spectroscopy. Infrared spectra were recorded on a 7199 B FT-IR system. UV−vis spectra were obtained with a Shimadzu 240 spectrophotometer. ^{1}H NMR spectra were measured on a Bruker ARX 400 using tetramethylsilane as an internal standard. Photoluminescence (PL) and electroluminescence (EL) spectra were measured with a Hitachi F-4500 fluorescence spectrophotometer. The PL quantum yield of a degassed dichloromethane solution of the Re complex was calculated using eq 1, where φ_s and φ_{std} are

$$\varphi_s = \varphi_{std}\frac{A_{std}}{A_s}\frac{I_s}{I_{std}}\frac{\eta_s^2}{\eta_{std}^2} \quad (1)$$

the quantum yields of unknown and standard samples ($\varphi_{std} = 0.042$ for [Ru(bpy)^3]$^{2+}$),[11] A_s and A_{std} (<0.1) are the solution absorbances at the excitation wavelength (λ_{ex}), I_s and I_{std} are the integrated emission intensities, and η_s and η_{std} are the refractive indices of the solvents.

Cyclic Voltammetry. Cyclic voltammetry measurements were conducted on a model CH 600 voltammetric analyzer with a platinum plate as the working electrode, a saturated calomel electrode (SCE) as the reference electrode, and a polished platinum wire as the counter electrode, at a scan rate of 0.1 V/s. The supporting electrolyte was 0.1 mol/dm^3 tetrabutylammonium hexafluorophosphate (TBAH) in CH$_3$CN. Prior to electrochemical measurements, the solution was deoxygenated with bubbling nitrogen for 15 min. Ferrocene was added at the end of each experiment to serve the internal reference. Its potential $E°$ was taken to be +0.425 V vs SCE.[12]

Crystallography. The crystals suitable for single-crystal X-ray analysis were obtained by slow evaporation of a dichloromethane−hexane solution. The data were collected at 18 °C on a CCD area detector Bruker SMART 2000 X-ray diffractometer with graphite-monochromatized Mo Kα radiation (λ = 0.71073 Å) in an $\omega-2\theta$ scanning mode. The 2θ range is 5.50−50.06°. The coordinates of all non-hydrogen atoms and anisotropic thermal parameters were refined by full-matrix least-squares. The data were processed on a Pentium PC using the Bruker SHELXTL software package.[13]

Electroluminescence. The electroluminescent device was fabricated in the following two-layer configuration: ITO/*N*,*N*′-diphenyl-*N*,*N*′-bis(3-methylphenyl)-1,1′-biphenyl-4,4′-diamine (TPD) (51 nm)/Re(CO)$_3$ClL (56 nm)/Mg$_{0.9}$Ag$_{0.1}$ (110 nm)/Ag (60 nm). The device was fabricated by sequential vacuum deposition of TPD and the Re complex from molybdenum crucibles at rates of 0.1−0.4 nm/s, and Mg:Ag alloy and Ag from tungsten wire baskets at rates of 0.1−1.0 nm/s onto an ITO-coated glass substrate below a pressure of 1×10^{-3} Pa without breaking vacuum. The layer thickness was controlled in a vacuum with an IL-1000 quartz crystal monitor and was also corrected by a Dektak[14] surface profile measuring system. The luminance was measured with a ST-86LA spot photometer and a close-up lens providing a focal spot of 5 mm at room temperature under ambient atmosphere.

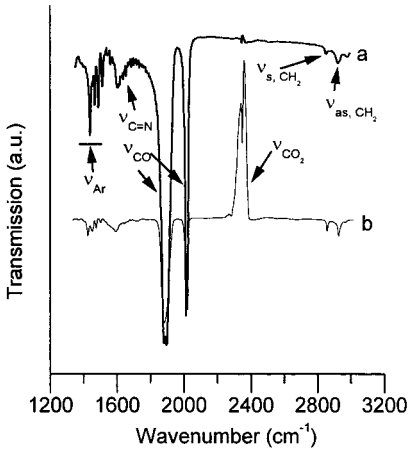

Figure 1. Infrared spectra of of the Re complex in KBr pellet (a) and vacuum-deposited film (b).

Results and Discussion

Infrared Spectroscopy. IR spectroscopy is a powerful tool to monitor the vacuum deposition behavior of materials.[15] The FTIR spectra for the Re complex in a KBr pellet and film are compared in Figure 1. The spectrum for the KBr pellet shows three CO stretching bands at 2019, 1895, and 1880 cm^{-1} which are consistent with the *fac* configuration at the rhenium center.[16] The former band appears at 2017 cm^{-1}, and the latter two bands appear as a single wide peak centered at 1889 cm^{-1} in the spectrum of a vacuum-deposited film on CaF_2. A heterocyclic C═N stretching band is observed at 1605 cm^{-1} for the KBr pellet[3c] and at 1604 cm^{-1} for the film. The aryl ring stretching bands at 1514, 1490, 1468, and 1440 cm^{-1} for the KBr pellet are almost unchanged compared to those (1514, 1489, 1467, and 1441 cm^{-1}) for the film. CH_2 antisymmetric and symmetric stretching frequencies are seen at 2916 and 2848 cm^{-1} for the film and at 2922 and 2852 cm^{-1} for the KBr pellet, respectively. These demonstrate stable vacuum deposition of the Re complex without significant thermal decomposition.

UV−Vis Spectroscopy. UV−vis spectroscopy has frequently been used to characterize vacuum-deposited films. In some cases, however, the UV−vis spectrum of the vacuum-deposited film could be largely deformed compared to the solution spectrum due to the light scattering caused by inhomogeneous film thickness and distribution of particle

(11) Rajendran, T.; Manimaran, B.; Lee, F. Y.; Lee, G. H.; Peng, S. M.; Wang, C. C.; Lu, K. L. *Inorg. Chem.* **2000**, *39*, 2016.
(12) (a) Gennett, T.; Milner, D. F.; Weaver, M. J. *J. Phys. Chem.* **1985**, *89*, 2787. (b) Cunha, C. J.; Dodsworth, E. S.; Monteiro, M. A.; Lever, A. B. P. *Inorg. Chem.* **1999**, *38*, 5399.
(13) Sheldrick, G. M. *SHELXS97 and SHELXL97, PC Version*; University of Göttingen: Göttingen, Germany, 1997.
(14) Kido, J.; Nagai, K.; Okamoto, Y. *J. Alloys Compd.* **1993**, *192*, 30.
(15) (a) Wang, K. Z.; Li, L. J.; Liu, W. M.; Xue, Z. Q.; Huang, C. H.; Lin, J. H. *Mater. Res. Bull.* **1996**, *31*, 993. (b) Wang, K. Z.; Xue, Z. Q.; Ouyang, M.; Zhang, H. X.; Huang, C. H. *Solid State Commun.* **1995**, *7*, 481.
(16) Giordano, P. J.; Wrighton, M. S. *J. Am. Chem. Soc.* **1979**, *101*, 2888.

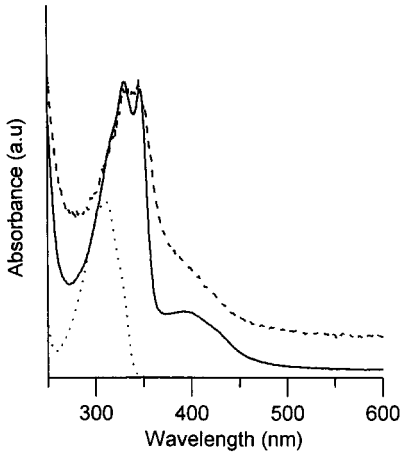

Figure 2. UV−vis spectra for the Re complex in a vacuum deposited film (dashed line) and chloroform solution (solid line), and for the ligand L in chloroform solution (dotted line).

dimensions.[17] Therefore one should be cautious in making any conclusion about the vacuum deposition stability of the materials solely relying on UV−vis spectroscopy. As shown in Figure 2, the ultraviolet absorption spectrum of the Re complex in $CHCl_3$ exhibits two peaks at 331 and 347 nm due to intraligand $\pi \rightarrow \pi^*$ transitions which are red-shifted compared to the broad absorption peak at 310 nm for free ligand L in $CHCl_3$ and are almost the same as those for the film (330 and 346 nm). The visible absorption spectrum of the chloroform solution appears as a broad absorption band centered at 400 nm which is ascribed to MLCT [$d\pi \rightarrow \pi^*$-(L)] transition and became ill-defined in the spectrum of the film. The film and the chloroform solution give almost the same onset absorption located at ∼481 nm, which corresponds to an energy difference of 2.58 eV between the highest occupied molecular orbital (HOMO) and the lowest unoccupied molecular orbital (LUMO).[18]

Crystallography. The crystallographic data for the Re complex are given in Table 1. Selected bond lengths and angles are given in Table 2. A perspective drawing of the structure of the complex with atomic numbering is shown in Figure 3. The Re and Cl atoms were found to be partially disordered and were split into two sites with occupancy factors of 0.8/0.2, respectively. This resulted in a comparatively high anisotropic temperature factor for terminal C(16). The coordination geometry at the Re atom is a distorted octahedron with the three carbonyl ligands arranged in a facial fashion. The average Re−C(CO) bond distance is 1.87(8) Å, and the average Re−N bond distance is 2.16(1) Å. The C−C bond distance for the bridgehead carbon atoms of the ligand L (C7−C8) is 1.47(2) Å, which is in agreement with that for the 2,2′-bipyrimidine congener.[19] The N(3)−C(8) bond length of 1.39 Å is reasonably longer than the N(2)−C(7) bond distance of 1.26 Å, indicating that the imidazole ring is much less conjugated than the pyridine ring

Table 1. Crystallographic Data

formula	$C_{17}H_{13}ClN_3O_3Re$
fw	528.95
color	yellow
cryst size, mm	0.30 × 0.20 × 0.15
cryst syst	orthorhombic
space group	*Pbca*
a, Å	12.713(6)
b, Å	15.103(7)
c, Å	18.253(8)
V, Å^3	3505(3)
Z	8
d_{calcd}, g, cm^{-3}	2.005
μ, mm^{-1}	7.108
F(000)	2016
$2\theta_{max}$, deg	50
reflns collected/unique	12486/2902 [*R*(int) = 0.1149]
abs correction	SADABS
T, K	298
GOF on F^2	1.001
R1, wR2 [$I > 2\sigma(I)$][a]	0.055, 0.1149
R1, wR2 (all data)[a]	0.1388, 0.1452
largest diff peak and hole, e Å^{-3}	+0.884, −0.952

[a] $R1 = \sum||F_o| - |F_c||/\sum|F_o|$; $wR2 = [\sum w(F_o^2 - F_c^2)^2/\sum w(F_o^2)^2]^{1/2}$.

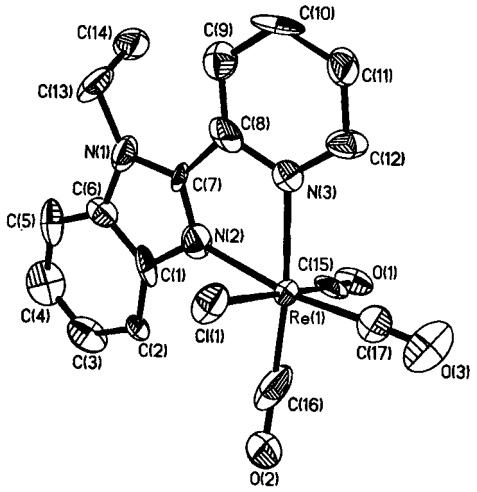

Figure 3. A perspective drawing of the Re(I) complex with atomic numbering scheme. Thermal ellipsoids are shown at the 50% probability level.

Table 2. Selected Bond Lengths (Å) and Angles (deg)

Re−N(2)	2.129(12)	Re−N(3)	2.184(7)
Re−Cl(1)	2.475(5)	Re−C(15)	1.92(2)
Re−C(16)	1.84(3)	Re−C(17)	1.848(19)
C(17)−Re(1)−C(16)	86.0(9)	C(16)−Re(1)−Cl(1)	93.3(8)
C(16)−Re(1)−C(15)	84.5(8)	C(15)−Re(1)−Cl(1)	175.1(4)
C(17)−Re(1)−C(15)	90.6(7)	N(2)−Re(1)−Cl(1)	86.6(4)
C(17)−Re(1)−N(2)	170.1(7)	N(3)−Re(1)−Cl(1)	81.6(3)
C(16)−Re(1)−N(2)	103.9(9)	Re(1)−C(17)−O(3)	175.0(17)
C(15)−Re(1)−N(2)	89.6(6)	Re(1)−C(16)−O(2)	179.0(2)
C(17)−Re(1)−N(3)	99.0(6)	Re(1)−C(15)−O(1)	177.0(14)
C(16)−Re(1)−N(3)	173.0(7)	C(15)−Re(1)−C(17)	90.6(7)
C(15)−Re(1)−N(3)	100.2(5)	C(16)−Re(1)−C(17)	86.0(9)
N(2)−Re(1)−N(3)	71.2(5)	C(15)−Re(1)−C(16)	84.5(8)
C(17)−Re(1)−Cl(1)	93.7(5)		

on the ligand L. The these two C(sp^2)−N(sp^2) bond lengths are also reasonably shorter than 1.45(2) Å for the C(13)-(sp^3)−N(1) (sp^3) bond length. The bond angles in Table 2 clearly indicate that CO ligands are linearly coordinated. The bond angles between adjacent CO carbon atoms are 84−90°, which is close to 90°, but the bond angle between the

(17) M. Uekawa, M.; Miyamoto, Y.; Ikeda, H.; Kaifu, K.; Nakaya, T. *Bull. Chem. Soc. Jpn.* **1998**, *71*, 2253.
(18) Robinson, M. R.; O'Regan, M. B.; Bazan, G. C. *Chem. Commun.* **2000**, 1645.
(19) Winslow, L. N.; Rillema, D. P.; Welch, J. H.; Singh, P. *Inorg. Chem.* **1989**, *28*, 1596.

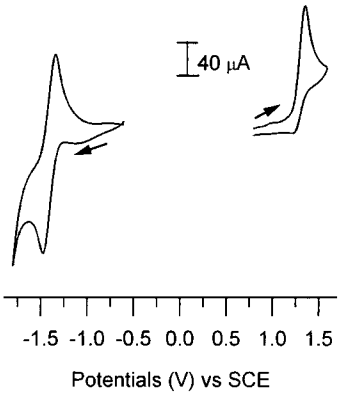

Figure 4. Cyclic voltammograms of the Re complex (CH_3CN/0.1 mol/dm^3 TBAH) at 0.1 V/s.

coordinated nitrogen atoms of ligand L is 71.2(5)°, which is much less than 90°. This is due not only to the steric requirement of the bidentate coordination of the ligand L19 but also to a twist of the imidazole ring relative to the pyridine plane. This twist is clearly verified by the fact that the normal to the plane of the pyridine ring intersects that of the imidazole ring at an angle of 6.5°. All other bond distances and angles are comparable to those found for the related rhenium(I) polypyridyl complexes.[11]

Cyclic Voltammetry. Cyclic voltammograms (Figure 4) of the Re complex show a couple of irreversible anodic waves at $E_{1/2} = 1.30$ V with an onset oxidation potential of +1.22 V vs SCE, and a couple of quasi-reversible cathodic waves at $E_{1/2} = -1.40$ V with an onset reduction potential of −1.32 V vs SCE. The anodic waves were associated with a Re^{I}-based oxidation process (Re^{I}/Re^{II}), and the cathodic waves with a L-based reduction process[20] ($[Re^{I}Cl(CO)_3(L)]/[Re^{I}Cl(CO)_3(L^{\bullet-})]^{-}$). From the onset oxidation (E_{onset}(Ox)) and reduction (E_{onset}(Red)) potentials, HOMO and LUMO energy levels of the Re complex were calculated (E_{HOMO} or E_{LUMO}/eV $= -4.74 - E_{onset}$(Ox) or E_{onset}(Red)) to be −5.96 and −3.42 eV with respect to the vacuum level, respectively, based on a calculated value of −4.74 eV for SCE with respect to the zero vacuum level.[21] The gap between the LUMO and the HOMO energy levels was thus derived to be 2.54 eV, which is well in agreement with that (2.58 eV) obtained from the UV−vis spectroscopy.

Photoluminescence and Electroluminescence. Photoluminescence (PL) spectra for the Re complex in compressed powder, vacuum-deposited film, and chloroform solution, and electroluminescence (EL) spectrum for the device ITO/*N*,*N*′-diphenyl-*N*,*N*′-bis(3-methylphenyl)-1,1′-biphenyl-4,4′-diamine (TPD) (51 nm)/$Re(CO)_3ClL$ (56 nm)/$Mg_{0.9}Ag_{0.1}$ (110 nm)/Ag (60 nm) are compared in Figure 5. Upon excitation of a degassed dichloroform solution of the Re complex at 400 nm, a PL quantum yield of 0.11% was obtained based on eq 1. In sharp contrast to the PL spectrum peaked at 363 nm ($\lambda_{ex} = 340$ nm) for ligand L in chloroform, PL maxima for the Re complex in the powder, vacuum-deposited film, and chloroform solution were found to be 550, 573, and 606 nm, respectively, while the electroluminescent device gave orange-red light emitting with the EL spectra depending on bias voltages. EL maxima were blue-shifted with increasing bias voltages (Figure 6), e.g., 600 nm for a bias voltage of 6 V and 586 nm for 10 V, indicating that the recombination of holes and electrons occurred in the Re complex layer and excitons produced subsequently excited the Re(I) complex. However, the obvious difference observed between the EL and PL spectra indicates that the electron-induced excited state is different from the photoinduced excited state. A small blue shift (≤10 nm) was also observed for a $Ru(bpy)_3(ClO_4)_2$-based electroluminescent device[7] when the bias voltages increased from 3.1 to 9.4 V, and a 12-nm blue shift was observed for a spin-coated film-based electroluminescent device with $Re(CO)_3Cl(mbpy)$ (mbpy = 4,4′-dimethylbipyridine) as the light-emitting layer upon the bias voltages increased from 1.5 to 6.5 V.[10c] The EL spectra for our electroluminescent device were red-shifted compared with the PL spectra for the powder and the vacuum-deposited film. The EL spectra, however, were blue-shifted at bias voltages

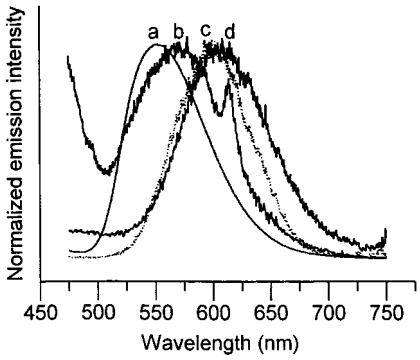

Figure 5. PL spectra for the Re complex in compressed powder (a), vacuum-deposited film (b), and chloroform solution (c), and EL spectrum for the device with a configuration of (+)ITO/TPD/$Re(CO)_3ClL/Mg_{0.9}Ag_{0.1}$/Ag(−) at a bias voltage of 6 V (d).

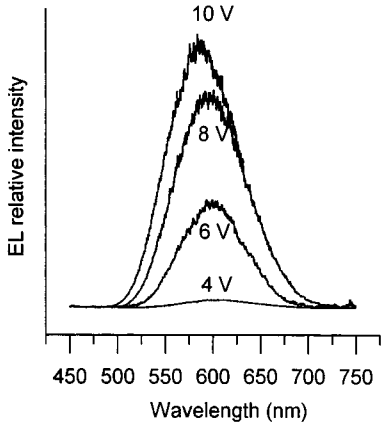

Figure 6. Bias voltage dependent EL spectra of the device with a configuration of (+)ITO/TPD/$Re(CO)_3ClL/Mg_{0.9}Ag_{0.1}$/Ag(−).

(20) (a) Berger, S.; Klein, A.; Kaim, W.; Fiedler, J. *Inorg. Chem.* **1998**, *37*, 5664. (b) Stor, G. J.; Hartl, F.; van Outersterp, J. W. M.; Stufkens, D. J. *Organometallics* **1995**, *14*, 1115. (c) Moya, S. A.; Guerrero, J.; Pastene, R.; Schmidt, R. Sariego, R. *Inorg. Chem.* **1994**, *33*, 2341. (d) Moya, S. A.; Pastene, R.; Schmidt, R.; Guerrero, J.; Sariego, R. *Polyhedron* **1992**, *11*, 1665. (e) Christesen, P.; Hammet, A.; Muir, A. V. G.; Timney, J. A. *J. Chem. Soc., Dalton Trans.* **1992**, 1455.

(21) (a) Bard, A. J.; Faulker, L. R. *Elctrochemical Methods—Fundamentals and Applications*; Wiley: New York, 1980. (b) Wu, D. G.; Huang, C. H.; Gan, L. B.; Zheng, J.; Huang, Y. Y.; Zhang, W. *Langmuir* **1999**, *15*, 7276. (c) Ashwini, K. A.; Samson, A. J. *Chem. Mater*. **1996**, *8*, 579.

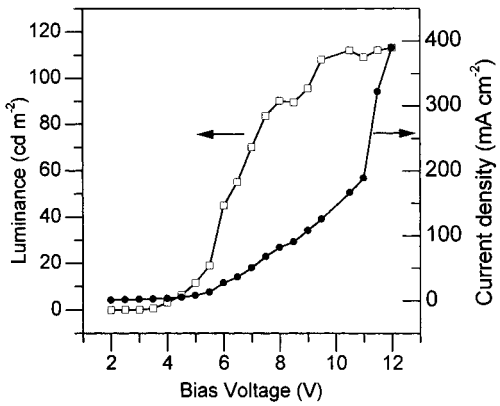

Figure 7. Current density−voltage and luminance−voltage curves of the device with a configuration of (+)ITO/TPD/$Re(CO)_3ClL/Mg_{0.9}Ag_{0.1}$/Ag(−).

equal to or lower than 8 V and almost the same at the bias voltages equal to or higher than 10 V, compared with the PL spectrum of the chloroform solution. Red shifts in the EL spectra compared with the PL spectra of the films were also observed for the $Re(CO)_3Cl$(mbpy)-based device.[10c] Also, a large red shift (50 nm) in the $Ru(bpy)_3(ClO_4)_2$-based EL spectra was observed relative to the acetonitrile and the aqueous solutions.[7]

A possible explanation for the relatively large variations observed between the EL and PL spectra of $Ru(bpy)_3(ClO_4)_2$ has been given as follows: electrons and holes were injected into the metal center and bpy ligand from the opposite electrodes, respectively, and electric field-driven electron and hole hopping occurred until these were localized on a single molecule producing the excited state of the Ru(II) complex.[7] In addition to this mechanism, formation of aggregates, interface energy transfer between the Re complex and TPD, and the change in the microenvironment of the Re complex induced by the applied electric field, as governed by the rigidochromism rule well-documented for the Re(I) complexes,[22] may be operative in our EL device. It is hard to make a definite conclusion at the present stage. The luminance−voltage and current density−voltage curves of the electroluminescent device are shown in Figure 7. It shows that the luminescence increased with increasing injection currents and bias voltages. The device exhibited a low turn-on voltage of ∼3 V and a rectification ratio greater than 10^4 at 12 V. The maximum external EL quantum efficiency[23] of 0.09% photons/electrons and luminous efficiency[23] of 0.9 lm/W were obtained at 6.0 V. At a bias voltage of 10.5 V and current density of 166 mA/cm^2, a maximum luminance of 113 cd/m^2 was achieved with a luminous efficiency of 0.2 lm/W and an external EL quantum efficiency of 0.03%. The maximum luminance for the present device is comparable to that of the EL devices we recently reported with Tb(III) and Eu(III) complexes as light-emitting layers.[4b,5] The maximum luminous efficiency is close to the level for the commercially available lighting diodes or ZnS-based EL devices.[3,24]

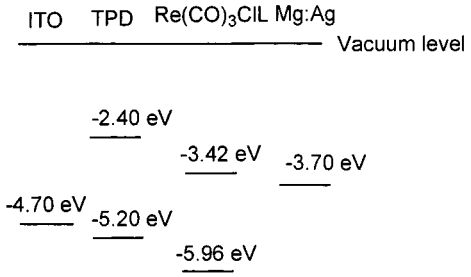

Figure 8. An energy level diagram of the EL device of (+)ITO/TPD/$Re(CO)_3ClL/Mg_{0.9}Ag_{0.1}$/Ag(−).

To best understand the device performance observed, an energy diagram for the EL device is given in Figure 8. The HOMO and LUMO energy levels for TPD and work functions for ITO anode and Mg:Ag cathode were taken from ref 4e. It is generally accepted that EL originates from the excitation of the light-emitting layer by the excitons produced by the recombination of electrons and holes which are injected from the cathode and the anode, respectively. The balanced injection and transport of holes and electrons are therefore crucial for achieving high quantum efficiency. It can be seen from Figure 8 that the barrier for electron injection from the Mg:Ag cathode to the Re complex layer is only 0.28 eV (the energy difference between the work function of Mg:Ag and LUMO of the Re complex), indicating that the Re complex we synthesized is a good electron transport material. The low turn-on voltage observed for the present EL device is due to the small barrier for electron injection from the Mg:Ag electrode to the Re complex layer. The barrier for electron injection from the Re complex to the TPD layer is as high as 1.02 eV. So, the TPD layer can effectively block the electrons so that the electrons injected from the Mg:Ag electrode can be effectively confined to the Re complex emitting layer. On the other hand, the barriers for hole injection from the ITO anode to the TPD layer and from the TPD layer to the Re complex layer are 0.52 and 0.76 eV, respectively, and these two values are much less than the barrier (1.26 eV) for direct hole injection from the ITO anode to the Re complex layer in a one-layer device of ITO/$Re(CO)_3ClL/Mg_{0.9}Ag_{0.1}$/Ag. Here the TPD played a role like a "ladder" in facilitating stepwise hole transport, similarly to Cu-phthalocyanine[25] and starburst molecues[26] which were used as buffer layers for hole injection in organic electroluminescent devices. In short, the TPD layer acted as both a hole transport and an electron-blocking layer, and the Re complex as an electron transport layer facilitating more balanced carrier injection from the anode and cathode.[3] This resulted in an increase in the recombination probability of electrons and holes in the Re complex layer and accordingly a reduction in the quenching probability of excitons created by the recombination of electrons and holes at the boundary

(22) (a) Lees, A. J. *Comments Inorg. Chem.* **1995**, *17*, 319. (b) Moya, S. A.; Guerrero, J.; Pastene, R.; Schmidt, R.; Sariego, R.; Sartori, R.; Sanz-Aparicio, J.; Fonseca, I.; Maertiez-Ripoll, M. *Inorg. Chem.* **1994**, *33*, 2341. (c) Lees, A. J. *Chem. Rev.* **1987**, *87*, 711.
(23) Mitschke, U.; Bauerle, P. *J. Mater. Chem.* **2000**, *10*, 1471.
(24) Abkowitz, M.; Pai, D. M. *Philos. Mag.* **1986**, *B53*, 193.
(25) Van Slyke, S. A.; Chen, C. H.; Tang, C. W. *Appl. Phys. Lett.* **1996**, *69*, 2160.
(26) Itano, K.; Ogawa, H.; Shirota, Y. *Appl. Phys. Lett.* **1998**, *72*, 636.

between the Re complex and the ITO electrode. As anticipated, the one-layer device without the hole transport TPD layer showed substantially low luminance.

In conclusion, a newly synthesized Re(I) complex was successfully applied for a vacuum-deposited film-based electroluminescent device. Bright orange-red light emitting with a low-voltage drive was demonstrated in the electroluminescent device. Good electroluminescent characteristics are due to rational design of the device configuation, and stable vacuum deposition and good electron transport properties of the Re complex. Efforts are being directed toward improving the hole transport and photoluminescent properties of the complexes.

Acknowledgment. This project was supported by the National Natural Science Foundation of China (20071004) and State Key Program of Fundamental Research (G1998061308), National Key Program for Fundamental Research (2001 CCD 04300), Beijing Natural Science Foundation (2002007), and Scientific Research Foundation for the Returned Overseas Chinese Scholars, State Education Ministry, to K.W..

Supporting Information Available: X-ray crystallographic file in CIF format for the structure determination of the Re(I) complex. This material is available free of charge via the Internet at http://pubs.acs.org.

IC0107330